A method to quantify the beneficial effect of scour protection on lateral behaviour of monopiles for offshore wind turbines

Li, Q.; Prendergast, L. J.; Gavin, K. G.; Askarinejad, A.; Wang, X. Q.

DOI
10.1016/j.oceaneng.2024.118196

Publication date
2024

Document Version
Final published version

Published in
Ocean Engineering

Ocean Engineering 307 (2024) 118196

Contents lists available at ScienceDirect

Ocean Engineering

journal homepage: www.elsevier.com/locate/oceaneng

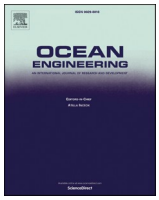

Research paper

A method to quantify the beneficial effect of scour protection on lateral behaviour of monopiles for offshore wind turbines

Q. Li [a,*], L.J. Prendergast [b], K.G. Gavin [c], A. Askarinejad [c], X.Q. Wang [d]

[a] PowerChina Huadong Engineering (Shenzhen) Corporation Limited, Shenzhen, 518100, China
[b] Department of Civil Engineering, Faculty of Engineering, University of Nottingham, Nottingham, NG7 2RD, United Kingdom
[c] Faculty of Civil Engineering and Geosciences, Delft University of Technology, 2628, CN, Delft, the Netherlands
[d] Department of Civil Engineering, Hangzhou City University, Hangzhou, 310015, China

ARTICLE INFO

Keywords:
Monopiles
Scour protection
Lateral loading behaviour
Slenderness ratios
Centrifuge tests
Finite element analyses

ABSTRACT

To mitigate against scour hole formation, scour protection can be placed around offshore wind turbine monopiles. Few studies have considered the beneficial effect of this geotechnical reinforcement measure on the foundation lateral resistance. The contribution of scour protection to lateral resistance of monopiles in sand is investigated in this paper using centrifuge tests and finite element analyses. Multiple scour protection widths and thicknesses are modelled around a monopile, to identify the most effective scour protection properties at mitigating lateral displacements. Two methods for modelling scour protection effects (one using material, the other using direct overburden pressure) are compared. The lateral response of monopiles with different slenderness ratios under various scour protection widths and overburden pressures are simulated. Results suggest that pile lateral displacements reduce by up to 41% when scour protection with width 2*D* (*D*, pile diameter) and applied overburden pressure of 30 kPa is used, compared to no scour protection, for a given test case. A method to modify design approaches to consider the beneficial contribution of scour protection on pile lateral behaviour using an envelope diagram is proposed, which provides relationships for scour protection properties and various monopile slenderness ratios.

1. Introduction

Monopiles are open-ended, steel tubular piles, with typically low slenderness ratios (*L/D*; *L*, pile embedded length; *D*, pile diameter). They are a proven cost-effective foundation solution for Offshore Wind Turbines (OWTs), and support more than 80% of all installed OWTs to date (Fan et al., 2019; Komusanac et al., 2022). Until a few years ago, the use of monopiles appeared limited to water depths of 30 m or less, with different foundation technology such as jackets or floating options being used for larger depths. In recent years, however, monopiles have continued to be installed in water depths exceeding even 50 m, suggesting this foundation type will remain popular for emerging new developments (Geoengineer.org, 2021).

The typical sizes of monopiles used to support early 2.5–5 MW OWTs had diameters between 4 and 6 m, with embedded lengths between 20 and 35 m, resulting in *L/D* ratios between 5 and 6 (Doherty and Gavin, 2012; Wu et al., 2019). With the continual evolution in OWT height to harness more energy per turbine, it has become necessary for monopile foundations to grow in size (Li et al., 2023), in order to resist the large overturning moments from environmental loads. As turbine capacities grow to 10 MW, the diameter required to limit pile groundline tilt must increase to between 8 and 10 m (Byrne et al., 2015). By comparison, OWTs are relatively lightweight structures so axial capacity tends not to be a governing design criterion, and as such embedded lengths of monopiles have not increased significantly. This is resulting in *L/D* ratios reducing from values of 5 to 6 towards values in the range 2–4 (Li et al., 2022).

Scour erosion of soil around marine structures is a well-recognised issue, mainly caused by local hydraulic actions due to the presence of the foundation influencing the water flow and wave characteristics, natural sediment transportation, and movement of bed features (Stride, 1982; Whitehouse et al., 2011). Scour can be particularly damaging to OWTs as it can alter the strength and stiffness of the foundation, impacting the dynamic stability (Prendergast et al., 2015, Prendergast et al., 2018), and ultimately affecting the fatigue life. After only six years

* Corresponding author.
E-mail addresses: qiangli1991@outlook.com (Q. Li), luke.prendergast@nottingham.ac.uk (L.J. Prendergast), K.G.Gavin@tudelft.nl (K.G. Gavin), A.Askarinejad@tudelft.nl (A. Askarinejad), wangxq@zucc.edu.cn (X.Q. Wang).

https://doi.org/10.1016/j.oceaneng.2024.118196
Received 5 March 2024; Received in revised form 30 April 2024; Accepted 13 May 2024
Available online 21 May 2024

List of notation

C_C	curvature coefficient of sand
C_U	uniformity coefficient of sand
c'_{ref}	(effective) cohesion
D	pile outer diameter
D_{50}	average grain size of sand
D_r	relative density of sand
D_s	scour depth
E	elasticity modulus
E_{ref}	reference stiffness
E_{50}^{ref}	secant stiffness for CD triaxial test
E_{oed}^{ref}	tangent oedometer stiffness
E_{ur}^{ref}	unloading reloading stiffness
e	loading eccentricity
e_{max}	maximum void ratio of sand
e_{min}	minimum void ratio of sand
f_m	lateral displacement ratio under 'material method'
f_s	lateral displacement ratio under 'stress method'
Gs	specific gravity of sand
g	gravitational acceleration rate
H	lateral load
h	water depth
I	moment of inertia
K_0^{nc}	K_0-value for normal consolidation
L	pile embedded length
M	mass
m	power of stress-level dependency of stiffness
P	symbol of length
p^{ref}	reference stress for stiffness
P_t	scour protection thickness
$P_{t,equ}$	equivalent scour protection pressure
P_w	scour protection width
R_f	failure ratio
T	time
t	pile wall thickness
y	lateral displacement
y_0	lateral displacement without scour protection
y_{ac}	actual lateral displacement with scour protection
y_m	lateral displacement under scour protection for 'material method'
y_s	lateral displacement under scour protection for 'stress method'
γ	unit weight of sand
δ	'material method' contact coefficient
ξ	final lateral displacement reduction factor
ψ	angle of dilation
$\boldsymbol{\theta}$	angle of pile tilt
$\boldsymbol{\zeta}$	lateral reinforcement factor
χ	variable for the selection of pressure
φ'	(effective) angle of internal friction
ν	Poisson's ratio
ν'_{ur}	Poisson's ratio for unloading-reloading
FEA	Finite Element Analyses
HS	Hardening Soil (constitutive model)
OWT	Offshore Wind Turbine

of operation, two monopiles at the Robin Rigg wind farm were decommissioned due to large unexpected scour development, which demonstrates the hazard posed to OWTs (Menéndez-Vicente et al., 2023). Scour holes usually form with larger depths in sandy deposits with an average scour depth 1.3D and a mean of 0.7D being observed in controlled tests (Sumer et al., 1992). For clay deposits, scour depths (D_s) typically vary between 0.75D and 1D (Kishore et al., 2008). Whitehouse et al. (2011) formulated a database of the scour development process and scour protection effectiveness, which contains data from approximately 115 piles at ten offshore wind farms. It was found that in 6 of the 115 cases, scour depths greater than or equal to the design value $D_s/D = 1.3$ were found, which is an alarming statistic showcasing the importance of addressing this problem.

To maintain structural stability, scour protection is required to prevent or reduce scour occurrence around offshore foundations (Li et al., 2024). Rock armour, rubble filter layers, solidified slurry, geotextile bags, and other materials can be used to cover a particular area of seabed surrounding the foundation with a certain thickness, which helps to mitigate the erosive action of currents, tides, and waves (Whitehouse, 1998; Heibaum, 1999; Lengkeek et al., 2017). A typical example schematic of a monopile foundation with scour protection installed on the seabed is shown in Fig. 1, where h refers to water depth, P_w refers to scour protection width, and P_t refers to scour protection thickness. For medium diameter monopiles (D = 4–5 m), scour protection with a width of 1.5-2D and with thickness in the range of 1.5–2.2 m is often used (Whitehouse et al., 20111). The effectiveness of scour protection options against scour erosion progression has been studied by several researchers (Whitehouse et al., 2011; Nielsen et al., 2013; Petersen et al., 2015). However, limited research has focussed on the structural capacity gained by scour protection. Of this limited research, Askarinejad et al. (2022) suggested that a scour protection layer with width of 2D and equivalent surcharge pressure of 15 kPa could increase foundation lateral capacity by 30%. Furthermore, they suggest the accumulation of

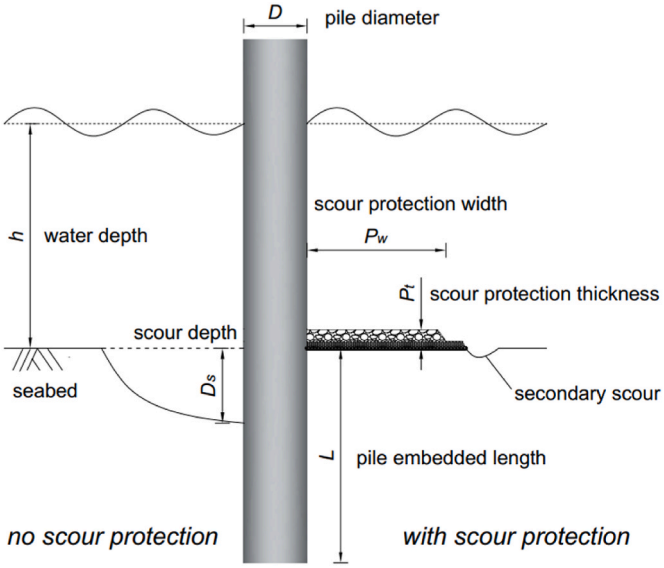

Fig. 1. Schematic illustration of monopile foundation without and with scour protection arrangement.

lateral deflection could be decreased by over 100%. While encouraging, no studies to date have focussed on developing systematic approaches to understanding the design requirements for scour protection layers that can improve pile lateral capacity in addition to combatting scour development, which is an important issue for the lifespan of monopile foundations.

The effect of various arrangements of scour protection layers on

monopile lateral behaviour is evaluated in this paper using centrifuge tests and Finite Element Analyses (FEA). Different parameters are considered, which includes the width and thickness of scour protection, the method of application, and the influence of pile slenderness ratio (L/D), on the resulting monopile lateral behaviour. The pile was considered to be embedded in homogeneous dense sand, and drained conditions are assumed to govern the lateral resistance, i.e. pore pressure accumulation is not considered. Using combined experimental and numerical analyses, a method to optimise monopile design to incorporate the beneficial effects of scour protection on pile lateral behaviour is proposed.

2. Experimental analysis

2.1. Geotechnical centrifuge and scaling factors

The geotechnical beam centrifuge at TU Delft is used in this work (Alderlieste, 2011). Including hardware and software changes, it has been continuously upgraded since 2009. Fig. 2 shows a photo of the setup in the latest configuration. The nominal diameter of the rotating arm is 2.5 m, and tests can be conducted at an operational limit of approximately 100g. Both of the test baskets have a maximum carrying capacity of 30 kg (Askarinejad et al., 2022; Li et al., 2020). For simulating pile-type structures in a geotechnical centrifuge, the normally observed scaling laws are summarized in Table 1.

2.2. Model pile and soil characterisation

A cylindrical aluminium pipe pile with outer diameter $D = 18$ mm and wall thickness $t = 1$ mm (at model scale) is used in this study. This open-ended pile has an embedded length $L = 90$ mm, leading to a slenderness ratio (L/D) of 5, representing typical values used for offshore foundations in recent years (Doherty and Gavin, 2012; Wu et al., 2019). The pile was manufactured using aluminium (instead of steel) in order to satisfy scaling surrounding the flexural rigidity. This enabled enlarging the pile wall thickness for the purpose of testing (Li et al., 2022). The primary pile dimensions and material properties are summarized in Table 2.

The absolute prototype dimensions of the pile in this study, namely the diameter, length, and wall thickness, are smaller than those used in practice for OWTs (Li et al., 2021). The reason for this lies with limitations in the testing capacity of the centrifuge, for example the limited size of the centrifuge basket and the associated strong box, and the limitation of the gravitational acceleration rate to 100g to protect electronic components. This does not pose an issue to the validity of the experimental results, however, as previous research has shown that

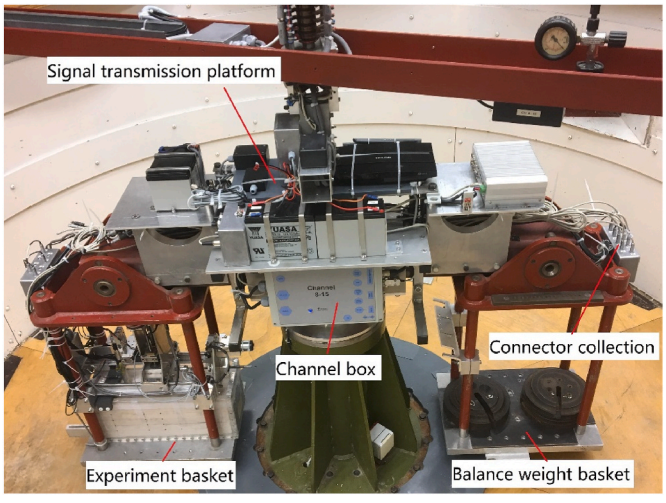

Fig. 2. Photo of the TU Delft centrifuge.

Table 1
Basic scaling laws for modelling of monopiles using centrifuge.

Physical quantity	Dimension	Similarity ratio (model/prototype)
Length	P	1:100
Time (dynamic)	T	1:100
Frequency	T^{-1}	100:1
Velocity	PT^{-1}	1:1
Acceleration	PT^{-2}	100:1
Area	P^2	$1:100^2$
Volume	P^3	$1:100^3$
Second moment of area	P^4	$1:100^4$
Mass	M	$1:100^3$
Flexural stiffness	MP^3T^{-2}	$1:100^4$
Force	MPT^{-2}	$1:100^2$
Stress	$MP^{-1}T^{-2}$	1
Strain	–	1

Table 2
Model and corresponding prototype pile dimensions and properties (Li et al., 2021).

Property	Model pile	Prototype pile[a]
Length (embedded + load eccentricity)	90 + 144 mm	9 + 14.4 m
Diameter, outer	18 mm	1.8 m
Wall thickness	1 mm	30 mm[a]
Elasticity modulus (E)	70 GPa	210 GPa[a]
Moment of inertia (I)	1936 mm^4	0.065 m^4
Bending stiffness (EI)	0.137 kPa m^4	13.7 GPa m^4

[a] Assuming prototype pile is fabricated from steel and centrifugal gravitational acceleration of 100g.

behaviour tends to be a function of pile slenderness rather than of the physical pile dimensions. The pile slenderness (rigidity, L/D) in this paper closely approximates that of real installed piles (Byrne et al., 2015, 2019; Li, 2020).

The artificial seabed was formulated using dry Geba silica sand with a relative density $D_r = 80\%$ using air pluviation. Pile outer diameter to mean particle size of the sand (D/D_{50}) ratio is 164, which can be considered large enough to avoid the particle size effect (Li et al., 2020). Pile wall thickness to mean particle size of the sand (t/D_{50}) ratio is 9.1, which is very close to the limiting value of 10 suggested by De Nicola (1996) and De Nicola and Randolph (1997), facilitating realistic interaction between the soil and the pile annulus (Li et al., 2020). The minimum and maximum void ratios are determined to be 0.64 and 1.07, respectively. Basic geotechnical properties of Geba sand are provided in Table 3.

The influence of water was excluded in the centrifuge trials as, (i) the analyses are assumed drained, and (ii) special liquids are typically required to undertake analyses incorporating pore fluid presence in centrifuge tests. As the purpose of the testing is to investigate relative influences of various scour protection parameters on pile lateral (monotonic) behaviour, the absence of fluid only influences the effective soil weight, and as such is omitted to simplify the experimental setup (Li et al., 2020). A similar treatment methodology was adopted by Klinkvort and Hededal (2013), LeBlanc et al. (2010), Li et al. (2010), Mu et al. (2018), and Verdure et al. (2003).

2.3. Testing program

The geo-centrifuge uses a two-dimensional loading actuator to apply lateral loads (H) near the pile head, at a pre-determined eccentricity of e

Table 3
Soil properties of Geba sand (De Jager et al., 2017; Li et al., 2020).

D_{50} (mm)	C_U	C_C	G_s	$\varphi'(^\circ)$	e_{min}	e_{max}
0.11	1.55	1.24	2.67	34	0.64	1.07

= 8*D* above the original (unprotected) seabed surface, to mimic the aerodynamic and hydrodynamic lateral loading from combinations of wind, wave, and current actions. Applied loading can be measured using installed load cells on the system (HTC-SENSORS; TAL220; measuring range 100 N; sensitivity 0.05%). The lateral displacements of the pile were measured at two locations: the pile head, and at 1.7*D* above the original seabed surface. These two measurements make it possible to calculate the pile displacement at the original seabed surface. The pile testing arrangement is shown in Fig. 3.

Table 4 presents the data for the three centrifuge tests performed in this study: one test without scour protection, and two tests with scour protection. Two different scour protection widths, namely 2*D* and 3*D*, with an equivalent effective surcharge pressure of 15 kPa were selected (Askarinejad et al., 2022; Matutano et al., 2013). As with the seabed, Geba sand was also used in the centrifuge tests to formulate the scour protection layer and to create the relevant surcharge load. It is worth noting that in real engineering applications, large-sized material such as graded stone or gravel is usually used to form the scour protection layer to prevent potential damage from the hydrodynamic environment. However, as the influence of water and the actual scour hydraulic development process were not considered in this research, the discrepancy caused by material size and particle distribution within the scour protection layer on pile lateral response is assumed to be minimal. To create the scour protection, a sand pouring apparatus was used to pour sand on the seabed surface beginning at the pile's outer surface, to a specified radial distance away from the pile foundation. Sand was poured layer by layer until the whole scour protection structure reached the target thickness.

Each centrifuge test was conducted as follows: 1) the model monopile was installed into the sand by jacking at 1*g*; 2) depending on the engineering requirements, scour protection material is added (or not) to the seabed; 3) the centrifuge is spun up to 100*g* to generate the required stress conditions; and 4) the lateral loading is applied to the pile and responses are measured.

Table 4
Centrifuge test programme.

Test ID	Soil	Pile geometry	Scour protection width	Scour protection pressure
CT-1	Geba sand	$D = 1.8$ m,	0	–
CT-2	($D_r = 80\%$)	$L = 5D$	2*D*	15 kPa
CT-3		(prototype)	3*D*	15 kPa

3. Finite element analysis

3.1. Geometry

To investigate the mechanism behind the beneficial contribution of a layer of scour protection on pile lateral behaviour, PLAXIS 3D CE V20 was used to perform the FEA. Benefitting from the symmetry of the problem, half of the pile-soil system is modelled to reduce computational expense. Fig. 4 shows the typical mesh used in this study in both elevation and plan view. The shading plot in the soil domain shows the stress state. Blue signifies low stress levels, while red signifies high stress levels. When a lateral load is applied to the pile, the shading plots exhibit some difference in the soil states which reflects the change of the stress level.

The soil domain is 12*D* in length, 6*D* in width, and 10*D* in height. These dimensions are determined from initial trial analyses to be large enough to eliminate boundary effects on the FE solutions while ensuring they are small enough to minimise calculation time. A refined mesh was particularly used in the vicinity around the pile, and a coarser mesh was implemented close to the boundary. In this numerical simulation scheme, various pile slenderness ratios ($L/D = 5$, 4.75, 4.5, 4.25, 4) were modelled by changing the pile embedded length, while keeping the pile diameter constant. The pile had a diameter (*D*) of 1.8 m, and the loading eccentricity was kept constant at $e = 8D$ (14.4 m), to remain in keeping with the centrifuge tests. The pile could be regarded as 'wished-in-place', and the soil inside the pile was assumed fully coring as the pile installation process was not modelled.

To model the influence of the overburden pressure associated with

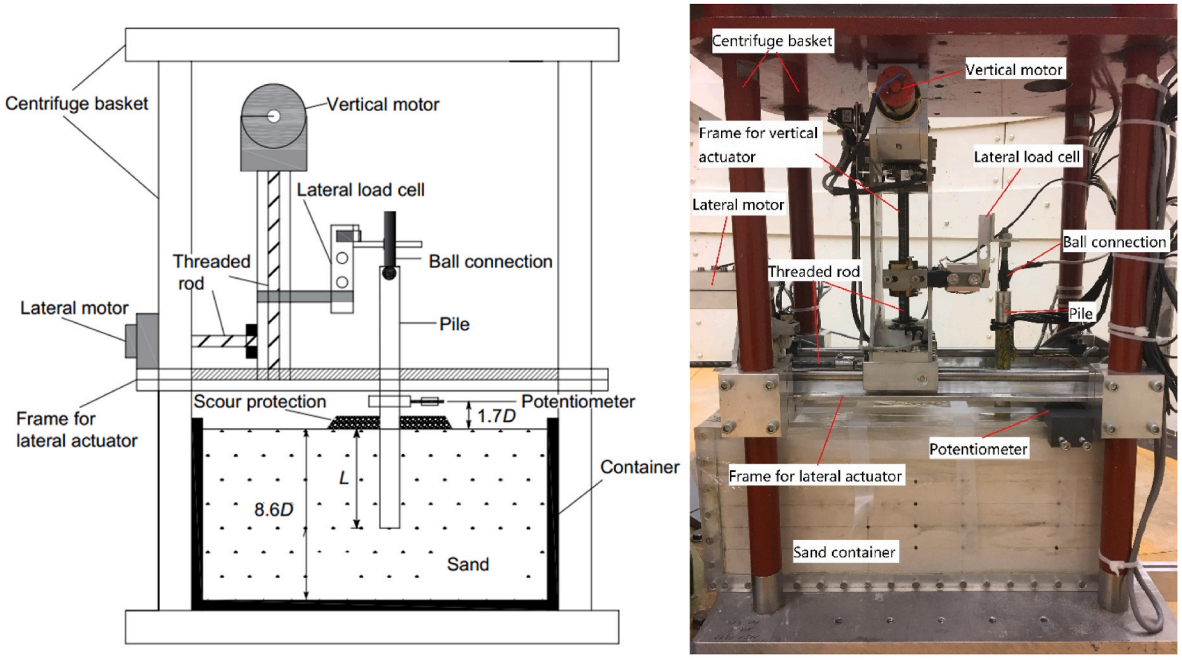

Fig. 3. Arrangement of actuator, pile and soil in the centrifuge basket: (a) Schematic diagram and (b) Photo.

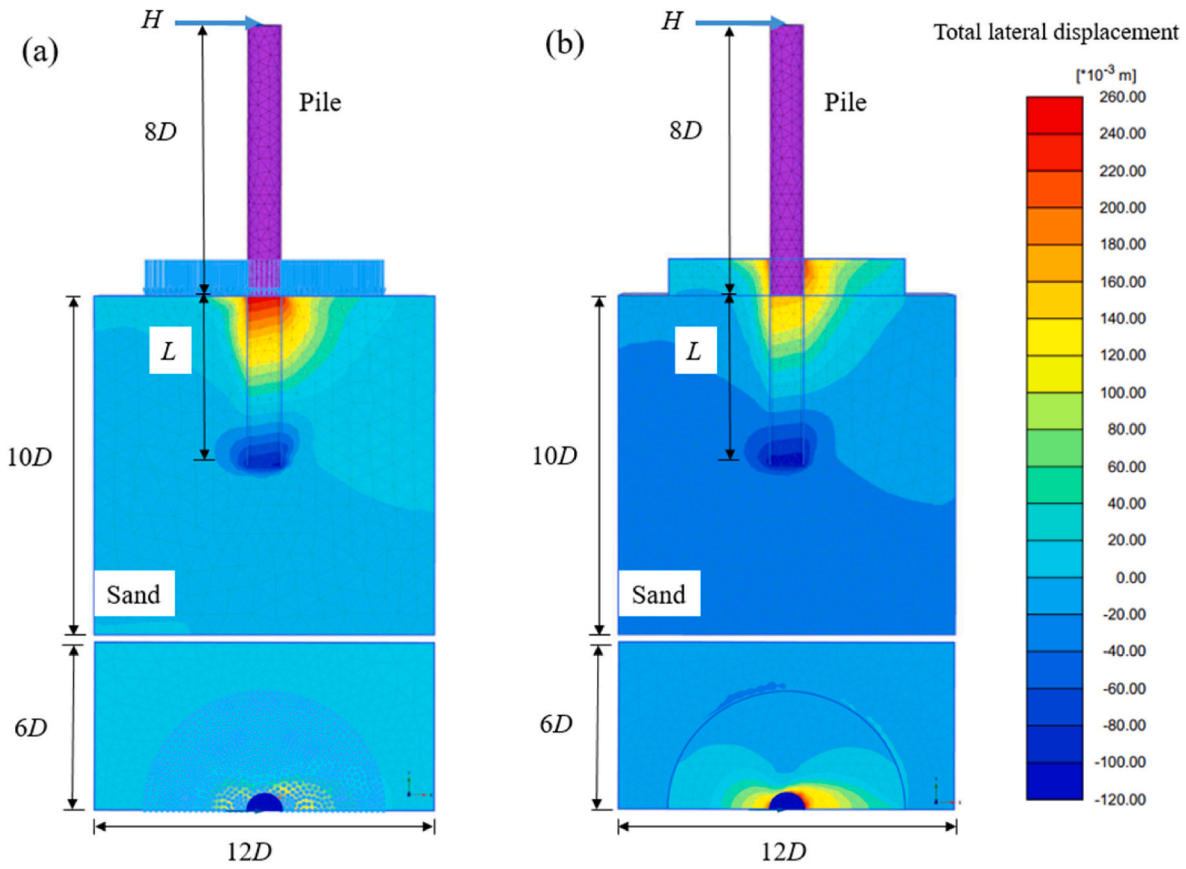

Fig. 4. The typical finite element model of the monopile under scour protection (elevation and plan): (a) 'stress method', and (b) 'material method'.

scour protection layers on the seabed, a strategy termed the 'stress method' was used previously by Askarinejad et al. (2022). The 'stress method' models the scour protection as an applied pressure in a circular area surrounding the pile, and ignores the physical contact between the pile column and the scour protection material. It should be noted, however, that in real environments, the material of the scour protection layer can deviate from the pile column (mobilizing no direct lateral resisting force to the pile), or it can adhere to the pile column (offering direct lateral resisting force to the pile), an effect that cannot be captured using the 'stress method' alone. In order to investigate the difference between these two specific pile-scour protection layer contacting cases, a method termed the 'material method' is implemented and compared with the 'stress method' in this work. The 'material method' considers an actual material layer in the model to create the surcharge pressure, and models the instance of full-adhesion between the pile column and the scour protection material. The scour protection layer was implemented on the seabed using the same seabed material with a certain thickness, distributed uniformly in a circular area around the monopile, with the same geometry as used in the centrifuge tests. Both the 'material method' and the 'stress method' can be considered as an upper-bound and lower-bound model for capturing the influence of the installed scour protection. Both modelling approaches are schematically shown in Fig. 4. It should be noted that a circular plate was artificially implemented on the exterior of the scour protection material in the FEA model for the 'material method' to maintain its shape for modelling purposes. In reality, a slope would be implemented at the edge of the boundary. This is not expected to adversely impact the results in this paper.

3.2. Soil model

The Hardening Soil (HS) model (Schanz, 1998), with nonlinear stress-dependant behaviour (Hicks and Wong, 1988), was adopted in this study to simulate the constitutive relationship of drained Geba sand used to formulate the seabed and scour protection layer. When primary deviatoric loading is applied, soil exhibits a decreasing stiffness and develops simultaneously unrecoverable plastic strains (Brinkgreve et al., 2016; PLAXIS, 2016). The axial strains and deviatoric stresses through triaxial loading is described by a hyperbolic formulation. The failure ratio R_f is set as a cut-off of the asymptotic behaviour of the hyperbolic formulation and R_f is normally taken as 0.9. The unloading-reloading stress path stiffness E_{ur}, as well as the primary loading stiffness E_{50}, is defined by the following constitutive equation:

$$E_x = E_x^{ref}\left(\frac{c \bullet \cos\varphi - \sigma_3' \bullet \sin\varphi}{c \bullet \cos\varphi + P_{ref} \bullet \sin\varphi}\right)^m \quad (1)$$

from which x denotes either the unloading-reloading stiffness (E_{ur}), or the secant elastic modulus at half of the deviatoric stress (E_{50}). This expression relies on: i) a pressure reference P_{ref}; ii) a reference stiffness E_{ref}, which is usually chosen as 100 kPa; and iii) a power exponent m, which is a rate of stress dependency and is usually taken as 0.5 for sands (Abril C, 2017).

For the calibrated set of material parameters (i.e. c'_{ref}, φ', ψ, m, E_{50}^{ref}, E_{oed}^{ref}, E_{ur}^{ref}, ν'_{ur}), a best-fit curve was created based on a parameter determination procedure proposed originally by Brinkgreve et al. (2010). The detailed derived and calibrated set of parameters for the HS model can be found in Li et al. (2024), while are briefly summarized in Table 5. A comparison between the numerical model implementing these calibrated parameters, and the results from centrifuge tests, is shown in section 4.3. The pile was assumed to be fabricated from steel and exhibits linear elastic material behaviour with $E = 210$ GPa and $\nu = 0.3$.

Table 5
Parameters used in the HS model (modified after Li et al. (2024)).

Name	γ	c'_{ref}	φ'	ψ	E_{50}^{ref}	E_{oed}^{ref}	E_{ur}^{ref}	m	ν'_{ur}	p^{ref}	R_f	K_0^{nc}
Value	15.57	0	34	4	1.6×10^4	1.6×10^4	4.8×10^4	0.45	0.2	100	0.9	0.4408
Unit	kN/m^3	kN/m^2	°	°	kN/m^2	kN/m^2	kN/m^2	–	–	kN/m^2	–	–

3.3. Parametric case studies

To ascertain the most effective geometries of scour protection on pile lateral bearing behaviour, and to maintain consistency with the centrifuge tests, four scour protection widths (i.e. $P_w/D = 1, 2, 3, 4$) and three scour protection thicknesses (i.e. $P_t = 1, 2, 3$ m) were modelled. The material of the scour protection layer was assumed to have a unit weight of 15 kN/m^3 in order to provide an equivalent surcharge to that in the centrifuge tests. It should be noted that for the cases implementing the 'stress method', the thickness of scour protection was substituted by an equivalent scour protection overburden pressure $P_{t,equ}$ (i.e. $P_{t,equ} = 15$, 30, 45 kPa), to remain in keeping with the stress generated by the overburden material in the model implementing the 'material method'. To investigate if it is possible to reduce the embedded pile length by taking advantage of the increased capacity afforded by the presence of the scour protection, pile lateral loading behaviour under reduced slenderness ratios (i.e. $L/D = 4.75, 4.5, 4.25, 4$) with installed scour protection was modelled, and compared to the case of the pile with slenderness ratio of 5 without scour protection. Dry sand was simulated in all of the FEA to maintain consistency with the centrifuge tests.

The FEA were performed in the following phases: i) the initial stress state due to the self-weight of the seabed was generated using soil elements; ii) the monopile was formed using shell elements and 'wished in place'; iii) the mechanism of scour protection was activated, either by activating the overburden pressure upon the seabed in the specified area (i.e. the 'stress method'), or by activating the soil elements inside the scour protection geometry (the 'material method'); iv) lateral loading was applied to the pile head and increased iteratively according to specified loading intervals. An overview of the FEA programme is presented in Table 6.

4. Analysis and results

In this section, the results of the centrifuge and FEA modelling are presented. All results (both measured and computed) are presented in prototype scale unless stated otherwise. The FEA in this section is performed on a pile with slenderness ratio (L/D) of 5. The pile lateral displacement is presented at the original (unscoured) seabed level.

Table 6
FEA programme (modified after Li et al. (2024)).

Test ID	Methodology	Pile Slenderness Ratio (L/D)	Scour Protection Width	Scour Protection Pressure/Thickness
FEA-0	–	5	–	–
FEA-1	Stress method	5	1D	15/30/45 kPa
FEA-2	Stress method	5	2D	15/30/45 kPa
FEA-3	Stress method	5	3D	15/30/45 kPa
FEA-4	Stress method	5	4D	15/30/45 kPa
FEA-5	Material method	5	1D	1/2/3 m
FEA-6	Material method	5	2D	1/2/3 m
FEA-7	Material method	5	3D	1/2/3 m
FEA-8	Material method	5	4D	1/2/3 m
FEA-9	Stress method	4.75	1D/2D/3D/4D	5/10/15/20/25/30 kPa
FEA-10	Stress method	4.5	1D/2D/3D/4D	10/20/30/40/50/60 kPa
FEA-11	Stress method	4.25	1D/2D/3D/4D	15/30/45/60/75/90 kPa
FEA-12	Stress method	4	1D/2D/3D/4D	20/40/60/80/100/120 kPa

4.1. Influence of scour protection on pile lateral load-displacement behaviour

Fig. 5 presents the numerical simulation results of the lateral load-displacement behaviour for the pile with different scour protection widths, simulated using the 'stress method' (signified with 'pressure, kPa') and using the 'material method' (signified with 'thickness, m'). In these figures, the nonlinear lateral load-displacement response is evident, and the nonlinearity reduces at higher applied pressures from the scour protection. At a given lateral load, the pile lateral displacement is observed to decrease with higher values of scour protection pressure. This phenomenon is enhanced as scour protection width increases from 1D to 4D.

From Fig. 5, it can be seen that although the amount of added pressure to the subsoil is the same for both the 'material method' and the 'stress method', the response of the pile under the 'material method' exhibits distinctly smaller lateral displacements than those observed under the 'stress method', for a given applied load. This difference becomes more significant at larger scour protection widths, thicknesses, and pressures. Under the 'material method', the added scour protection material has the effect of enlarging the pile embedment length, and this is likely to be the main reason for smaller lateral displacements than those observed under the 'stress method'.

To provide a direct comparison of the effect of the scour protection width on the pile lateral load-displacement behaviour, the data presented in Fig. 5 using the 'stress method' is rearranged and plotted in Fig. 6 to demonstrate the influence on increasing the scour protection width around the pile. For a given lateral load, the pile lateral displacement decreases with the increase of scour protection width. As scour protection pressure is increased from 15 kPa to 45 kPa, this effect becomes more prominent. It appears that the initial application of scour protection with width varying between 1D and 2D leads to the most significant decrease in the lateral displacement, suggesting that the scour protection functions most efficiently in increasing lateral resistance within a zone of width 2D around the pile.

4.2. Influence of scour protection on pile lateral capacity

From the previous analyses, the presence of scour protection reduces pile lateral displacements for a given applied load in all investigated conditions, i.e. for all scour protection pressures, widths, and thicknesses. Due to the load control characteristics of the FEA program, the effect of scour protection on the pile lateral behaviour can be conveniently evaluated using Lateral Displacement Ratios for stress method f_s and material method f_m according to the following equations:

$$f_s = y_s / y_0 \tag{2}$$

$$f_m = y_m / y_0 \tag{3}$$

whereas y_s and y_m denote lateral displacement under scour protection for 'stress method' and 'material method' respectively, and y_0 denotes lateral displacement under no scour protection.

From Fig. 6, it can be seen that at a lateral load corresponding to $H =$

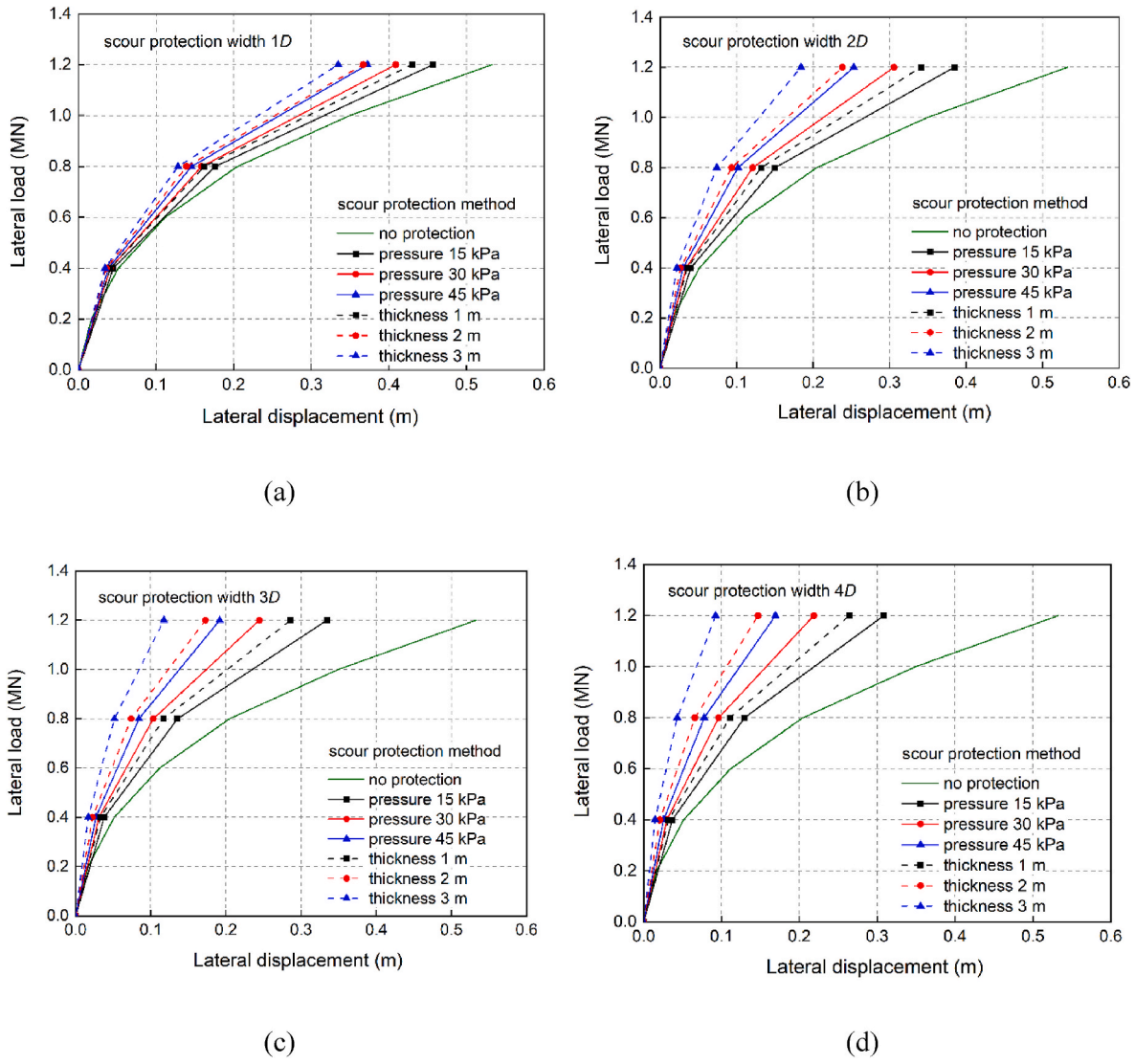

Fig. 5. Lateral load-lateral displacement relationships under four scour protection widths from FEA: (a) 1*D*, (b) 2*D*, (c) 3*D*, and (d) 4*D*.

0.8 MN, the pile lateral displacement with no scour protection is $y = 0.205$ m, approximately 0.11*D*. To facilitate comparison of bearing behaviour, Lateral Displacement Ratios f_s and f_m were all calculated at a consistent lateral load of $H = 0.8$ MN in the subsequent analyses, as 0.11*D* is close to the typically accepted lateral displacement criteria of 0.1*D* for determining pile lateral capacity (Li et al., 2020).

Fig. 7 shows Lateral Displacement Ratios f_s and f_m considering the influence of scour protection pressure, thickness, and width, using both the 'stress method' (signified with 'pressure, kPa') and the 'material method' (signified with 'thickness, m'). Increasing the scour protection pressure, thickness, and width decreases Lateral Displacement Ratios f_s and f_m. The trend is somewhat nonlinear in both cases. Overall, the pile Lateral Displacement Ratio under the 'material method' (f_m) shows a similar trend to that of the 'stress method' (f_s), but with smaller magnitudes. The initial application of scour protection pressure (from 0 to 15 kPa) and scour protection thickness (from 0 to 1 m) leads to the most significant decrease in Lateral Displacement Ratio. At a scour protection width of 2*D*, the application of scour protection thickness from 1 m to 2 m to 3 m using the 'material method' reduces the lateral displacement ratio f_m by 0.354 to 0.542 to 0.638 of the value under no scour protection. By comparison, the 'stress method' reduces f_s by 0.266 to 0.408 to 0.502 for the same conditions. The reduced Lateral Displacement Ratios under the 'material method' (f_m) is 12.0%, 22.7% and 27.2% smaller than under the 'stress method' (f_s).

In all applied scour protection pressure and thickness scenarios (Fig. 7(b)), apparent turning points can be observed on the Lateral Displacement Ratio, f_s and f_m, vs scour protection width curves. The secant stiffness of Lateral Displacement Ratio, f_s and f_m, vs scour protection width curves between 0 and 2*D* is about 3 times that between 2*D* and 4*D*. This implies the scour protection is most effective within a 2*D* width area in terms of increasing capacity. The effect of the scour protection shows a decreasing trend from a width of 2*D* to 4*D* from the pile, eventually becoming less effective outside 4*D* from the pile. The higher the scour protection pressure, the larger the curvature of the Lateral Displacement Ratio, f_s and f_m, vs scour protection width curves, which reflects the lateral load-displacement phenomenon observed in Fig. 6.

In summary, there is evidence to suggest that 2*D* (±1*D*) and 1 m–2 m (or 15–30 kPa) could be taken as an efficient estimate of scour protection width and thickness (or scour protection pressure) ranges to maximise the benefit to the lateral resistance properties of the piles tested in this analysis. From previous experimental investigations of scour protection geometries resisting wave-current induced scour, Du (2021) pointed out that the most effective scour protection width should cover the outer edge of the scour hole (that would occur if there were no scour protection), and this value for small diameter piles is approximately 3*D*, and for large diameter piles reduces to 2*D*. Combining the findings of the

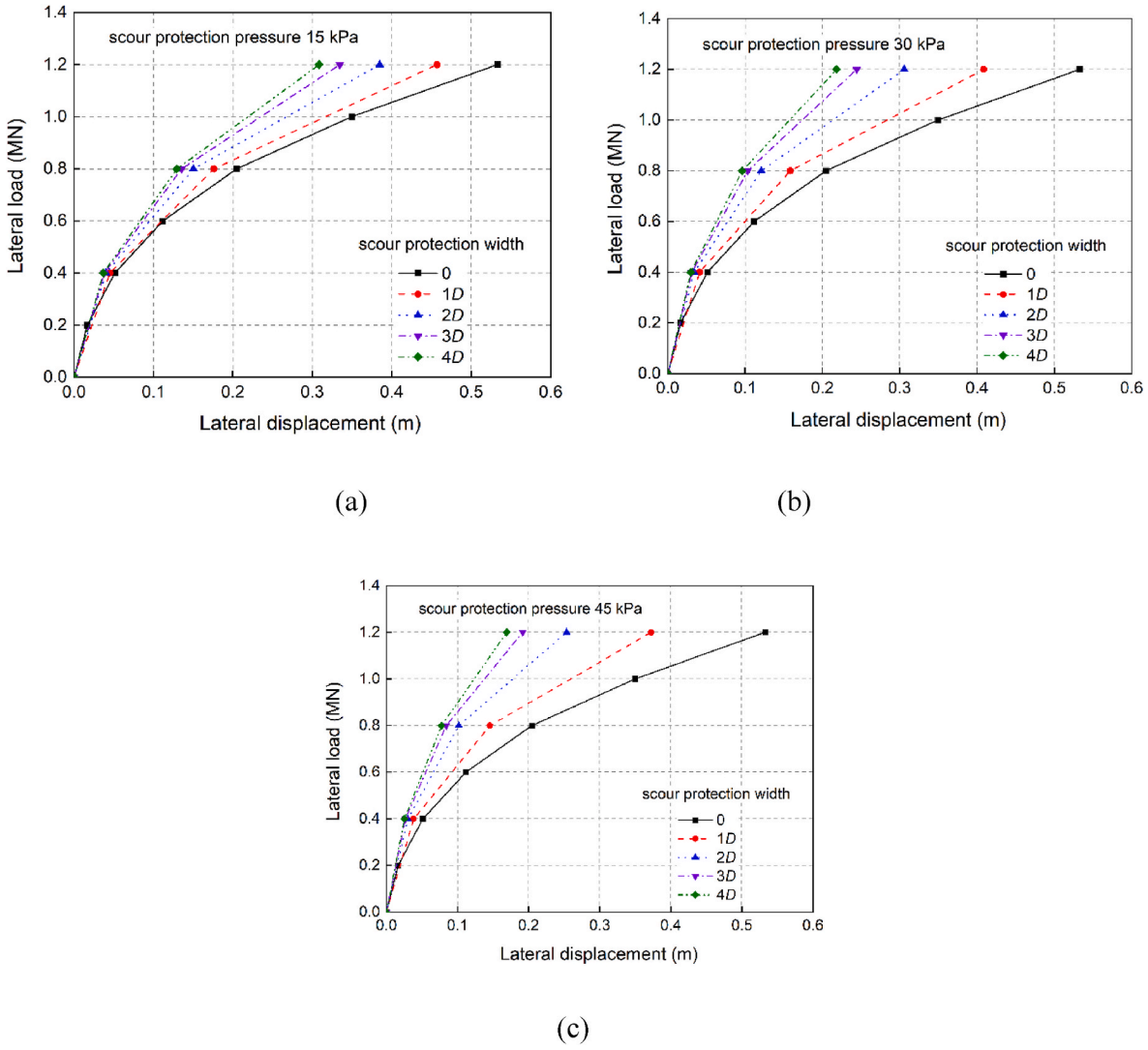

Fig. 6. Lateral load-lateral displacement relationships under three scour protection pressures using the 'stress method': (a) 15 kPa, (b) 30 kPa and (c) 45 kPa.

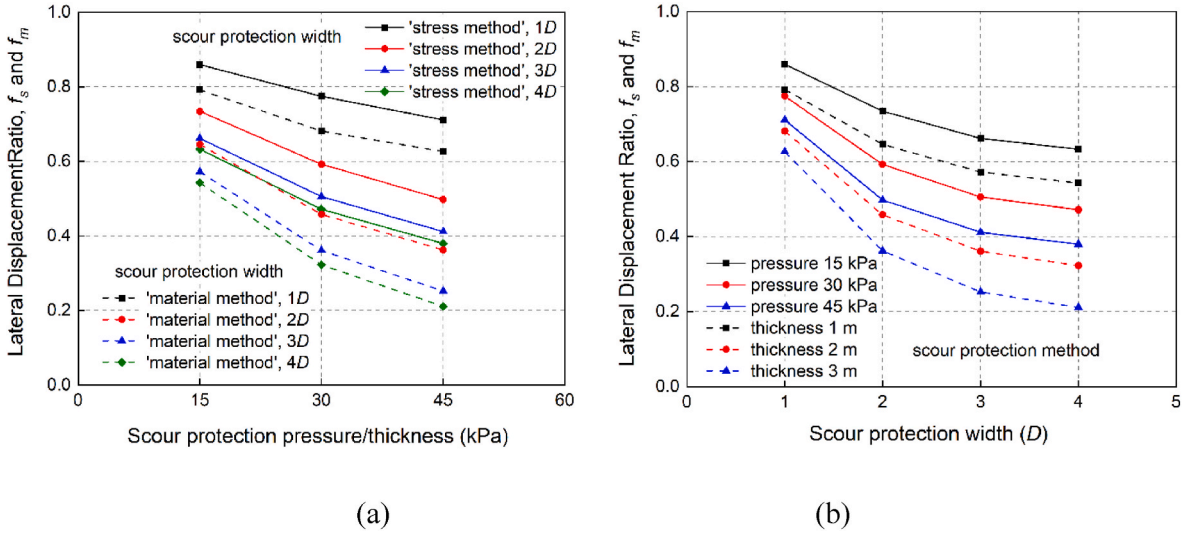

Fig. 7. Lateral Displacement Ratio f_s and f_m considering the effect of: (a) scour protection width, and (b) scour protection pressure and thickness.

present research together with the analysis of Du (2021) facilitates the provision of scour protection geometries to minimise scour development and maximise pile lateral capacity.

The FEA model can be used to help understand the underlying mechanism governing how scour protection enhances lateral behaviour of piles. An analysis of the mean effective stress profiles was undertaken herein under the cases of implementing the stress and material methods for modelling scour protection, at a given applied lateral load $H = 0.2$ MN. Fig. 8(a,b,d,f,h,j,l) present the mean effective stress ($\sigma_m^{'}$) for the case without scour protection and with the application of various scour protection pressures using the 'stress method'. Comparing Fig. 8(a,b,f,j, l), the mean effective stress in the soil beneath the scour protection area increased by around 3% with the increase of the scour protection width. By comparing Fig. 8(f and l), it can be observed that increasing the width of scour protection from 2*D* to 4*D* has little influence on augmenting the mean effective stress in the soil, but rather only impacts a larger area. Comparing Fig. 8(d–f and h) the mean effective stress beneath the scour protection increased by around 2%, 4%, and 6% as scour protection pressure was changed from 15, 30–45 kPa, which offers an explanation for the decrease of pile lateral displacement observed in Fig. 5.

Fig. 8(c,e,g,i,k,m) present $\sigma_m^{'}$ compared with the application of various scour protection scenarios using the 'material method'. Comparing both the 'material method' and the 'stress method', the influenced area and change in mean effective stress of the sub-soil from both strategies appears very similar. Additionally, the implemented scour protection layer directly provides lateral resistance to the pile, which is likely to be the main reason for the larger reduction in pile lateral displacement observed under the 'material method'.

4.3. Combined modelling approaches for scour protection effect on pile lateral behaviour

From the FEA, the 'material method' contributes more significantly to the pile lateral resistance than the 'stress method', as a means for modelling scour protection. Both the material and stress method are simplifications in themselves, i.e. it is unrealistic to assume no lateral resistance is provided to the pile as per the 'stress method', nor for full adhesion to occur as per the 'material method'. In the real case, scour protections is formulated using stone, gravel and sand, which is disorganized in the actual engineering construction process. Gaps and voids exist in between the pile structure and the scour protection material, which will influence the adhesion properties. In the real scenario, the effect of scour protection enhancing pile lateral resistance will be somewhere between that modelled using the 'stress method' and 'material method'.

Herein, a 'material method' contact coefficient δ is introduced to quantify the contact effectiveness of the pile structure with the scour protection layer. The value of δ varies between 1 and 0: $\delta = 1$ represents full material contact, equating to the 'material method'; and $\delta = 0$ represents non-material contact, equating to the 'stress method'. Depending on how much adhesion is expected for given materials and conditions, the estimation of contact effectiveness between the pile column and the scour protection layer can be modelled by choosing an appropriate δ value.

The pile actual lateral pile displacement with scour protection can be expressed by the following equation:

$$y_{ac} = y_0 f_s \left[1 - \delta\left(1 - \frac{f_m}{f_s}\right)\right] = y_0 f_s (1 - \delta\zeta) \tag{4}$$

where, y_{ac} denotes actual lateral displacement under scour protection, y_0 denotes lateral displacement without scour protection, f_s denotes Lateral Displacement Ratio by the 'stress method', and f_m denotes Lateral Displacement Ratio by the 'material method'. Lateral reinforcement factor ζ ($\zeta = 1 - \frac{f_m}{f_s}$) describes the extra decrease of Lateral

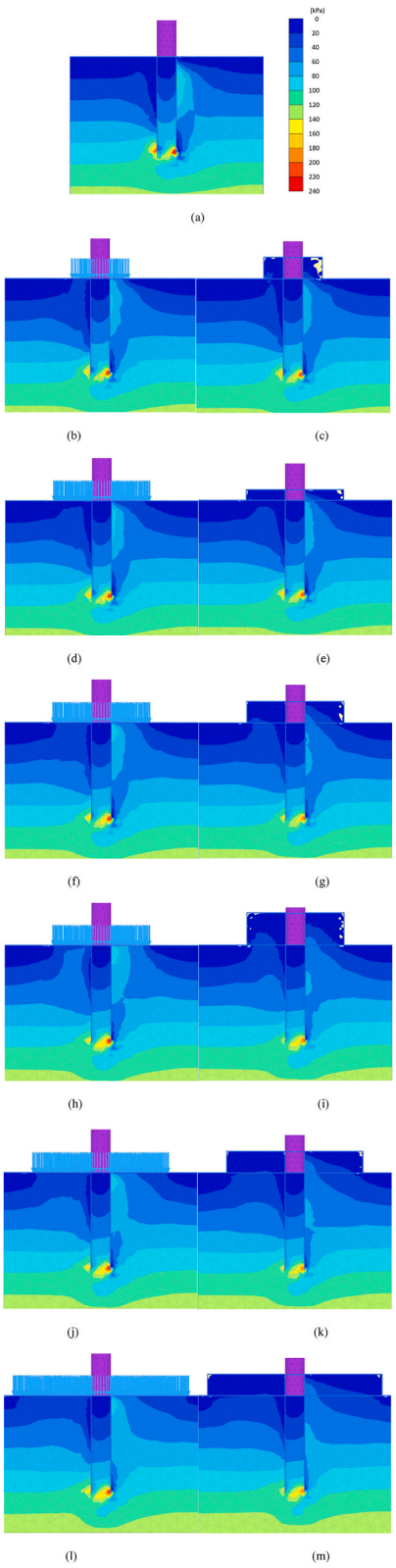

Fig. 8. Mean effective stress ($\sigma_m^{'}$) in the seabed before and after applying scour protection. Note: 1) Figures share the same legend; 2) (b, d, f, h, j, l), 'stress method'; 3) (c, e, g, i, k, m), 'material method'; 4) Void in plot means stress in tension state; 5) Lateral load $H = 0.2$ MN. (a) $P_w = 0$, $P_t = 0$; (b) $P_w = 1D$, $P_t =$ 30 kPa; (c) $P_w = 1D$, $P_t = 2$ m; (d) $P_w = 2D$, $P_t = 15$ kPa; (e) $P_w = 2D$, $P_t = 1$ m; (f) $P_w = 2D$, $P_t = 30$ kPa; (g) $P_w = 2D$, $P_t = 2$ m; (h) $P_w = 2D$, $P_t = 45$ kPa; (i) P_w $= 2D$, $P_t = 3$ m; (j) $P_w = 3D$, $P_t = 30$ kPa; (k) $P_w = 3D$, $P_t = 2$ m; (l) $P_w = 4D$, $P_t =$ 30 kPa; (m) $P_w = 4D$, $P_t = 2$ m.

Displacement Ratio by the 'material method' compared with the 'stress method'. The ζ values under the various investigated scour protection conditions are given in Table 7.

From Table 7, it can be seen that the lateral reinforcement factor ζ increases with the increase of scour protection width, thickness, and pressure. Lateral reinforcement factor ζ shows an overall average value of 0.221 under all investigated scour protection conditions, which implies the lateral displacement simulated under the 'material method' is on average 22.1% smaller than that simulated under the 'stress method', which is notable. Under low values of scour protection thickness and pressure (1 m/15 kPa, specifically), ζ shows an average value of 0.12. Under large scour protection thickness and pressure (3 m/45 kPa, specifically), ζ shows an average value of 0.306. Therefore, the beneficial effects of scour protection material on decreasing pile lateral displacement under large scour protection thickness (and pressure) should be considered in design, as there are potential economic benefits.

The data measured in the centrifuge (CT-1, CT-2, CT-3) and computed in the FEA (FEA-0; FEA-2, FEA-3 at scour protection pressure 15 kPa; FEA-6, FEA-7 at scour protection thickness 1 m) are compared in Fig. 9, which shows lateral load-displacement relationships for piles. The FEA model provides a reasonable match to the overall development of pile lateral displacement with lateral load compared with the centrifuge test case without scour protection (i.e. FEA-0 vs. CT-1). The good agreement between the computed and measured results suggests the reliability of calibrated material parameters of the HS model. Comparing the lateral load-displacement behaviour of the centrifuge data with scour protection width 2D and without scour protection, the decrease of pile lateral displacement could be as high as 30% at a lateral load of 0.8 MN. When increasing the scour protection width from 2D to 3D, the change of overall lateral load-displacement behaviour of the centrifuge test data is about 10%.

The centrifuge test results for the various scour protection cases provide an intermediate response between those of the FEA for both the 'material method' and the 'stress method'. This suggests the necessity of introducing the 'material method' contact coefficient δ in evaluating the extra beneficial contribution of scour protection by the 'material method', compared to the 'stress method' on pile lateral behaviour. A 'material method' contact coefficient of $\delta = 0.65$ can be approximately estimated from Fig. 9, which satisfies both scour protection widths of 2D and 3D. This value is used in a design example in the subsequent section. It should be noted that this value is specific to the conditions investigated in the present study, and for alternative materials and conditions, a similar experimental analysis would be required.

According to design practice, monopiles for OWTs must be capable of resisting 10^8 to 10^9 aerodynamic and hydrodynamic load cycles (from wind, wave, and currents) of varying direction, amplitude, and frequency at a proposed site over an operational lifetime of 20–30 years (Liu, 2020). To fulfil relevant serviceability limit state requirements, a maximum permanent rotation of a monopile (monopile tilt) at mudline of 0.5° is permitted (DNV, 2016). Considering the pile geometry and rotation point located at around 0.8L below the original seabed surface, $\theta = 0.5°$ corresponds to a mudline displacement of $y = 0.063$ m (i.e., 0.035D), which is significantly smaller than the $y = 0.1D$ lateral capacity criterion. This displacement occurs at a corresponding lateral load H of 0.4 MN, see Figs. 5 and 9, for the case without scour protection in this paper. When comparing the scour protection effect on the lateral bearing behaviour at an applied $H = 0.4$ MN, the absolute values of y are smaller compared with those obtained at $H = 0.8$ MN under different scour protection cases. However, the influence of scour protection enhancing the lateral resistance remains true.

Table 7
Lateral reinforcement factor, ζ

Scour protection width	Scour protection thickness/pressure			Average
	1 m/15 kPa	2 m/30 kPa	3 m/45 kPa	
1D	0.079	0.121	0.119	0.106
2D	0.120	0.227	0.272	0.206
3D	0.136	0.286	0.387	0.269
4D	0.143	0.316	0.445	0.301
Average	0.120	0.237	0.306	0.221

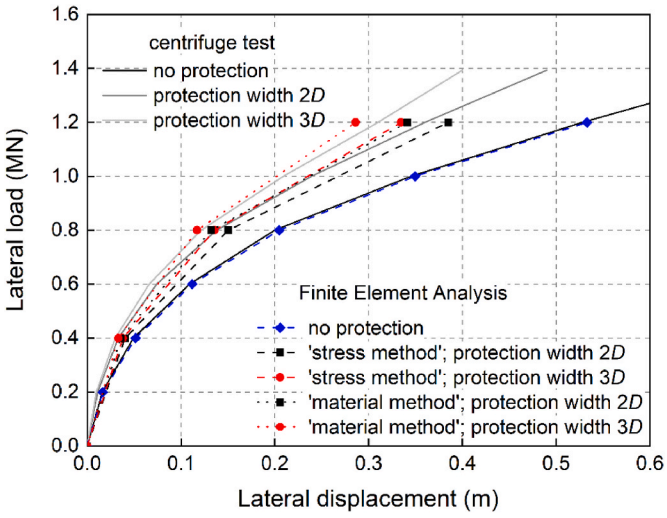

Fig. 9. Measured and computed lateral behaviour of monopiles considering effect of scour protection.

4.4. Method to calculate reduced lateral displacement under scour protection

A design example is undertaken herein to demonstrate the operation of Eq. (4) in deriving the expected reduction in pile lateral displacement under the presence of scour protection. For this example, a rigid monopile with $L/D = 5$ is assumed to be installed in dense sand (D_r = 80%). The task relates to determining the actual pile lateral displacement (y_{ac}) under scour protection thickness $P_t = 1.6$ m and scour protection width $P_w = 2.2D$, using a 'material method' contact coefficient δ = 0.65. The scour protection material possesses a unit weight of $\gamma = 14$ kN/m^3. Under certain design conditions, the lateral displacement of the monopile without scour protection is predetermined to be $y_0 = 10$ cm for the purposes of this numerical demonstration.

Firstly, it is necessary to convert scour protection thickness P_t (=1.6 m) to equivalent scour protection pressure $P_{t,equ}$:

$$P_{t,equ} = \gamma P_t = 14\times1.6 = 22.4 \text{ kPa} \quad (5)$$

Assuming a scour protection width 2.2D and equivalent pressure 22.4 kPa, the pile Lateral Displacement Ratio f_s (by 'stress method') can be obtained from Fig. 7(b) using interpolation, which gives 0.64. The lateral reinforcement factor ζ can be obtained from Table 7 using interpolation, which yields 0.181.

Accordingly, the pile actual lateral displacement (y_{ac}) can be calculated using Eq. (4), as follows:

$$y_{ac} = y_0 f_s(1 - \delta\zeta) = 10\times0.64\times(1 - 0.65\times0.181) = 10\times0.565 = 5.65 \text{ cm} \quad (6)$$

In summary, by applying such a scour protection measure and assuming a 'material method' contact coefficient δ = 0.65, the pile lateral displacement would decrease by 43.5% to 5.65 cm. From the design point of view, the pile design methodology could be modified to achieve a more economical design, e.g. using a reduced length pile, which is discussed in the next section.

5. Modification of pile design methodology to incorporate beneficial effects of scour protection

5.1. Design envelopes

The application of a scour protection layer can effectively improve the lateral bearing capacity of existing monopile foundations, which implies that shorter piles might be useable in certain design scenarios to achieve the same lateral bearing response with the aid of scour protection. Therefore, more FEA is needed to explore the relationship among scour protection thickness (pressure), scour protection width, and pile length on maintaining the original pile resistance in the absence of scour protection. Herein, four groups of numerical simulations (FEA-9, FEA-10, FEA-11 and FEA-12 listed in Table 6) were performed using the 'stress method', with each group containing 25 distinct scour protection conditions: i) no scour protection; ii) coupling of scour protection widths $P_w/D = 1, 2, 3, 4$ and scour protection pressures $P_t = \{5, 10, 15, 20, 25, 30\}^*\chi$ kPa. χ can be taken as 1, 2, 3, and 4 for the piles with L/D ratios of 4.75, 4.5, 4.25, and 4 respectively.

The acquisition of the envelope diagram for monopile design considering properties of the scour protection layer is introduced herein. Firstly, FEA-0, a pile with an L/D ratio of 5 without scour protection, was set as the reference simulation, from which a lateral displacement of $y = 0.205$ m was obtained at corresponding lateral load of $H = 0.8$ MN. Subsequently, a pile with L/D of 4.75 (FEA-9) was created, with varying scour protection widths (1D, 2D, 3D, and 4D). For each width, the scour protection pressure was increased until the lateral displacement of the pile was the same as the reference pile ($L/D = 5$) with no scour protection. A hyperbolic relationship of scour protection width vs scour protection pressure for the pile with $L/D = 4.75$ was therefore obtained. In short, this curve shows the combined values of scour protection width and pressure that are required to result in the same lateral displacement as the longer pile with no scour protection.

Subsequently, following the same methodology, the scour protection width vs scour protection pressure relationships for piles with L/D ratios of 4.5, 4.25, and 4 (FEA-10, FEA-11, and FEA-12) were obtained. This data is plotted together in Fig. 10. Note, the curves shown in Fig. 10 stipulate the lower-bound limit of the scour protection width and scour protection pressure combinations, or in other words, the lower-bound limit of the pile L/D ratios (the smallest pile L/D ratios that could satisfy the capacity). Data for piles with L/D varying between the values in Fig. 10 can be obtained via interpolation.

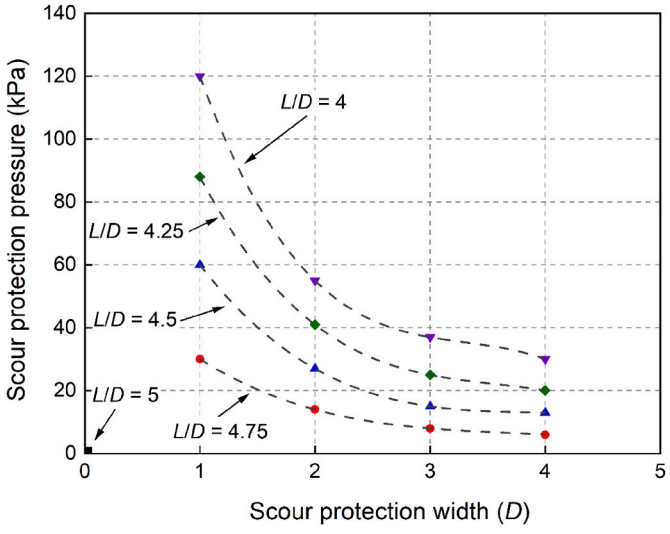

Fig. 10. Envelope diagram of monopile design considering properties of scour protection layer (using the 'stress method').

5.2. Case application

An example is provided herein to demonstrate the use of the envelope diagram for monopile design incorporating the beneficial contribution of scour protection. Consider a rigid monopile ($L/D = 5$) that has already been designed according to traditional methods, i.e. all the pile properties (e.g. material, geometry) and installation method have been determined. The pile is assumed to be installed in a dense sand seabed, and scour protection is not considered initially.

The tasks are: i) to determine the pile slenderness ratio (L/D) required incorporating scour protection with thickness $P_t = 1.6$ m, and width $P_w = 2.2D$, using the 'stress method', where the scour protection material has a unit weight of $\gamma = 14$ kN/m^3; ii) when assuming a 'material method' contact coefficient $\delta = 0.65$, provide suggestions on optimizing the pile design considering scour protection 'material effect'.

Firstly, based on an equivalent scour protection pressure of 22.4 kPa (calculated by Eq. (5)) and scour protection width 2.2D, a pile slenderness ratio $L/D = 4.6$ can be found from Fig. 10 by interpolation. The deduced pile slenderness ratio in the last procedure is relatively safe, as the lateral resistance provided directly by scour protection material is not in consideration. The design example shown in section 4.4 and some crucial parameters (e.g. lateral reinforcement factor, ζ; Lateral Displacement Ratio by stress method, f_s; Lateral Displacement Ratio by material method, f_m) are based on a pile with an L/D ratio of 5, however, the theoretical implication and the calculated results are worth being referred to. Therefore, lateral reinforcement factor ζ of a pile with slenderness ratio $L/D = 4.6$ could be taken as 0.181 herein as a trial analysis.

From Table 7 and Equation (4), pile final lateral displacement reduction factor ξ considering the influence of 'material method' could be determined by the following equation:

$$\xi = \delta\zeta = 0.65 \times 0.181 = 0.118 \tag{7}$$

Analysis indicates that by considering the scour protection pressure effect, the pile slenderness ratio (L/D) has been reduced from 5 to 4.6. Moreover, the pile slenderness ratio has some potential for further reduction. The reason lies in that under the design lateral load $H = 0.8$ MN, the original pile lateral displacement ($y = 0.205$ m) could experience a reduction of 11.8% benefiting from the extra lateral resistance provided directly by the scour protection layer, i.e. the 'material method'. It implies that the selected pile has the potential for further shortening, or the pile reserves a greater safety margin.

6. Conclusions

In this paper, the effect of scour protection on the lateral behaviour of OWT monopiles was investigated using geotechnical centrifuge tests and Finite Element Analyses. Scour protection has a beneficial impact on pile lateral behaviour, and the influence varies according to the modelling strategy adopted. By harnessing the beneficial aspects, pile designs may be optimised to take the presence of scour protection into account. The following key conclusions are summarized:

1. The presence of scour protection was observed to significantly decrease pile lateral displacements under given applied loads. At a scour protection width 2D and applied scour protection pressure of 30 kPa, lateral displacement reduces by 41% compared with the case of no scour protection, for the given pile properties studied. For economical purposes, 2D ($\pm$1D) and 1 m–2 m could be taken as a suitable scour protection width and thickness range in engineering applications for monopile foundations.
2. The presence of scour protection not only provides the subsoil with overburden pressure, but also directly offers lateral resistance to the monopile. When using the 'material method', the added scour protection material has an effect of enlarging the effective pile embedment length, causing the Lateral Displacement Ratios under the

'material method' to be on average 22.1% smaller than those under the 'stress method', which is a marked difference.

3. 'Material method' contact coefficient δ can be incorporated into the pile design methodology, in order to reflect the effectiveness of the 'material method' compared with the 'stress method' in decreasing pile lateral displacements. The results between centrifuge tests and FEA show overall good agreement, which suggests the calibrated material parameters of the HS model used in this paper are reliable.
4. Envelope diagrams of monopile optimization design are derived by integrating the relationships of scour protection width, pressure, and pile slenderness ratio. Superimposing the beneficial effect of scour protection, a pile with reduced embedded length can be used that maintains the same bearing capacity as the original longer unprotected pile.

There are some limitations in the approach and recommendations for further research. The physical process of scour is sensitive to different seabed sediment environments. The scour rate and optimum scour depth can be high in sandy non-cohesive soils and lower in clayey soils. However, only one soil stratum, i.e. a sand deposit, is investigated in this research. Sophisticated conditions could occur if surface layer thickness has a limiting effect (e.g. thin layer of clay overlying sand), or thin layer of fine sand overlying clay. In addition, the thickness of a surface layer (sand or clay) could have an effect on the development of scour. Assessing the effectiveness of scour protection in heterogeneous soils should be carried out. In addition, further studies are also encouraged to expand the investigation to the influence of scour protection on pile lateral behaviour under cyclic loading, and for cases where scour protection is added some time after a scour hole has developed, as a remedial measure.

The overall lateral extent of scour around a pile in a sandy seabed is typically 4-5D without placed protection. A well-planned scour protection strategy can be effective in protecting monopile foundations from scour, and secondary scour (at the edge of the protection) is normally very limited in depth and area adjacent to the placed scour protection. Therefore, the effect of secondary scour is not considered in this research but may have some influence. If secondary scour develops to a noteworthy scale, its influence on the scour protection layer and on the pile lateral loading behaviour should be evaluated.

Sand material was used to formulate the scour protection layer. It should be noted that this is a deviation from the real engineering application, whereby silt solidified by polyurethane or stone armour is frequently used. The contact coefficient δ might be different among various scour protection materials. Larger roughness or cohesion will lead to a higher contact coefficient δ. From Table 7, scour protection material with larger effective unit weight has the same impact as larger scour protection thickness/pressure, which can lead to a higher reinforcement factor ζ. However, the methodology for determining the contact coefficient δ and reinforcement factor ζ follows that as demonstrated in this paper.

CRediT authorship contribution statement

Q. Li: Writing – original draft, Methodology, Investigation, Formal analysis, Data curation, Conceptualization. **L.J. Prendergast:** Writing – original draft, Validation, Software, Methodology, Data curation. **K.G. Gavin:** Writing – review & editing, Supervision, Resources, Project administration, Funding acquisition. **A. Askarinejad:** Writing – review & editing, Visualization, Supervision, Software, Resources. **X.Q. Wang:** Writing – review & editing, Visualization, Supervision, Methodology, Funding acquisition.

Declaration of competing interest

The authors declare the following financial interests/personal relationships which may be considered as potential competing interests:

Qiang Li reports financial support was provided by Zhejiang Engineering Research Centre of Intelligent Urban Infrastructure (IUI2023-ZD-02). Xinquan Wang reports financial support was provided by National Natural Science Foundation of China (NSFC) (Grant No.52278373). Qiang Li reports financial support was provided by China Scholarship Council (CSC). Remaining authors declare that they have no known competing financial interests or personal relationships that could have appeared to influence the work reported in this paper.

Data availability

Data will be made available on request.

Acknowledgements

This research is supported by National Natural Science Foundation of China (NSFC) (Grant No.52278373) and Zhejiang Engineering Research Centre of Intelligent Urban Infrastructure (IUI2023-ZD-02). The first author would like to express gratitude to China Scholarship Council (CSC) and to the Section of Geo-Engineering, Delft University of Technology.

References

Abril, C.A.M., 2017. Numerical Simulations of Static Liquefaction in Submerged Slopes. Master dissertation. Delft University of Technology, Delft, the Netherlands.
Alderlieste, E.A., 2011. Experimental Modelling of Lateral Loads on Large Diameter Monopile Foundations in Sand. Master dissertation. Delft University of Technology, Delft, the Netherlands.
Askarinejad, A., Wang, H., Chortis, G., Gavin, K., 2022. Influence of scour protection layers on the lateral response of monopile in dense sand. Ocean Eng. 244, 110377.
Brinkgreve, R.B.J., Engin, E., Engin, H., 2010. Validation of empirical formulas toderive model parameters for sands. 7th European Conference Numerical Methods in Geotechnical Engineering (Numge 2010), Trondheim 1, 137–174.
Brinkgreve, R.B.J., Kumarswamy, S., Swolfs, W., 2016. 3D PLAXIS Manual. Delft, Netherlands.
Byrne, B.W., Mcadam, R., Burd, H.J., Houlsby, G.T., Martin, C.M., Gavin, K., Doherty, P., Igoe, D., Zdravkovie, L., Taborda, D.M.G., Potts, D.M., Jardine, R.J., Sideri, M., Schroeder, F.C., Muir Wood, A., Kallehave, D., Skov Gretlund, J., 2015. Field testing of large diameter piles under lateral loading for offshore wind applications. Proc. XVI ECSMGE Geotech. Eng. Infrastruct. Dev. 1255–1260.
Byrne, B.W., Burd, H.J., Zdravkovic, L., McAdam, R.A., Taborda, D.M., Houlsby, G.T., et al., 2019. PISA: new design methods for offshore wind turbine monopiles. Rev. Fr. Geotech. 158, 3.
De Jager, R.R., Maghsoudloo, A., Askarinejad, A., Molenkamp, F., 2017. Preliminary results of instrumented laboratory flow slides. Elsevier Ltd., Delft, The Netherlands.
De Nicola, A., 1996. The Performance of Pipe Piles in Sand. Doctoral dissertation. University of Western Australia, Perth, Australia.
De Nicola, A., Randolph, M.F., 1997. The plugging behaviour of driven and jacked piles in sand. Geotechnique 47 (4), 841–856.
DNV, 2016. DNVGLST0126: support structures for wind turbines. Technical report, Osol, Norway, DNV GL.
Doherty, P., Gavin, K., 2012. Laterally loaded monopile design for offshore wind farms. Proc. Inst. Civ. Eng. Energy 165 (1), 7–17.
Du, S., 2021. Study on Local Erosion Characteristics and Solidified Soil Protection of Single Pile Foundation for Offshore Wind Power. Master dissertation, Southeast University, Nanjing, China.
Fan, S., Bienen, B., Randolph, M.F., 2019. Centrifuge study on effect of installation method on lateral response of monopiles in sand. Int. J. Phys. Model. Geotech. 1–13.
Geoengineer.org, 2021. Scottish offshore wind farm: monopile foundations to go beyond 50-metre depths. Available online: https://www.geoengineer.org/news/scottish-offshore-wind-farm-monopile-foundations-to-go-beyond-50-metre-depths. (Accessed 8 January 2024).
Heibaum, M.H., 1999. Coastal scour stabilisation using granular filter in geosynthetic nonwoven containers. Geotext. Geomembranes 17 (5–6), 341–352.
Hicks, M.A., Wong, S.W., 1988. Static liquefaction of loose slopes. Numer. Methods GeoMech. 1361–1367.
Kishore, Y.N., Rao, S.N., Mani, J.S., 2008. Influence of the scour on laterally loaded piles. The 12th International Conference of International Association for Computer Methods and Advances in Geomechanics, Goa, 1-6 October 3283–3288.
Klinkvort, R.T., Hededal, O., 2013. Lateral response of monopile supporting an offshore wind turbine. Proc. Inst. Civ. Eng. Geotech. Eng. 166 (GE2).
Komusanac, I., Brindley, G., Fraile, D., Ramirez, L., 2022. Wind energy in Europe (2021 statistics and the outlook for 2022-2026. Issue.
LeBlanc, C., Houlsby, G.T., Byrne, B.W., 2010. Response of stiff piles in sand to long-term cyclic lateral loading. Geotechnique 60 (2), 79–90.
Lengkeek, W., Didderen, K., Teunis, M., Driessen, F., Coolen, J.W.P., Bos, O.G., Vergouwen, S., et al., 2017. Eco-friendly design of scour protection: potential enhancement of ecological functioning in offshore wind farms: towards an

implementation guide and experimental set-up. Bureau Waardenburg, Culemborg 96.
Li, Q., 2020. Response of Monopiles Subjected to Combined Vertical and Lateral Loads, Lateral Cyclic Load, and Scour Erosion in Sand. PhD Thesis. Delft University of Technology, Delft, the Netherlands.
Li, Z., Haigh, S.K., Bolton, M.D., 2010. Centrifuge modelling of mono-pile under cyclic lateral loads. 7th International Conference on Physical Modelling in Geotechnics 2, 965–970.
Li, Q., Prendergast, L., Askarinejad, A., Chortis, G., Gavin, K., 2020. Centrifuge modeling of the impact of local and global scour erosion on the monotonic lateral response of a monopile in sand. Geotech. Test J. 43 (5).
Li, Q., Askarinejad, A., Gavin, K., 2021. The impact of scour on the lateral resistance of wind turbine monopiles: an experimental study. Can. Geotech. J. 58, 1770–1782.
Li, Q., Gavin, K., Askarinejad, A., Prendergast, L.J., 2022. Experimental and numerical investigation of the effect of vertical loading on the lateral behaviour of monopiles in sand. Can. Geotech. J. 59 (5), 652–666.
Li, Q., Chen, P., Gao, L., Meng, D., Zou, J., 2023. Influence of vertical load on lateral-loaded monopiles by numerical simulation. Comput. Model. Eng. Sci. 135 (1).
Li, Q., Wang, X., Gavin, K., Jiang, S., Diao, H., Wang, K., 2024. Influence of scour protection on the vertical bearing behaviour of monopiles in sand. Water 16, 215.
Liu, H., 2020. Constitutive Modelling of Cyclic Sand Behaviour for Offshore Foundations. PhD Thesis. Delft University of Technology, Delft, the Netherlands.
Matutano, C., Negro, V., Lopez-Gutierrez, J.S., Esteban, M.D., 2013. Scour prediction and scour protections in offshore wind farms. Renew. Energy 57, 358–365.
Menéndez-Vicente, C., López-Querol, S., Bhattacharya, S., Simons, R., 2023. Numerical study on the effects of scour on monopile foundations for Offshore Wind Turbines: the case of Robin Rigg wind farm. Soil Dynam. Earthq. Eng. 167, 107803.
Mu, L., Kang, X., Feng, K., Huang, M., Cao, J., 2018. Influence of vertical loads on lateral behaviour of monopiles in sand. Eur. J. Enviro. Civ. Eng.
Nielsen, A.W., Liu, X., Sumer, B.M., Fredsøe, J., 2013. Flow and bed shear stresses in scour protections around a pile in a current. Coast Eng. 72, 20–38.
Petersen, T.U., Sumer, B.M., Fredsøe, J., Raaijmakers, T.C., Schouten, J.J., 2015. Edge scour at scour protections around piles in the marine environment: laboratory and field investigation. Coast Eng. 106, 42–72.
PLAXIS, 2016. 2D-3-Material-Models.
Prendergast, L.J., Gavin, K., Doherty, P., 2015. An investigation into the effect of scour on the natural frequency of an offshore wind turbine. Ocean Eng. 101, 1–11.
Prendergast, L.J., Reale, C., Gavin, K., 2018. Probabilistic examination of the change in eigenfrequencies of an offshore wind turbine under progressive scour incorporating soil spatial variability. Mar. Struct. 57, 87–104.
Schanz, T., 1998. Zur Modellierung des Mechanischen Verhaltens von Reibungsmaterialen. Ph.D. thesis (in German). Stuttgart University, Stuttgart, Germany.
Stride, A. (Ed.), 1982. Offshore Tidal Sands, vol. 237. Chapman and Hall.
Sumer, B.M., Fredsøe, J., Christiansen, N., 1992. Scour around vertical pile in waves. J. Waterw. Port, Coast. Ocean Eng. 118 (1), 15–31.
Verdure, L., Garnier, J., Levacher, D., 2003. Lateral cyclic loading of single piles in sand. Int. J. Phys. Model. Geotech. 3 (3), 17–28.
Whitehouse, R.J.S., 1998. Scour at Marine Structures. Thomas Telford, London, p. 216.
Whitehouse, R.J.S, Harris, J.M., Sutherland, J., Rees, J., 2011. The nature of scour development and scour protection at offshore windfarm foundations. Marine Pollution Bulletin 62 (1), 73–88.
Wu, X., Hu, Y., Li, Y., Yang, J., Duan, L., Wang, T., Adcock, T., Jiang, Z., Gao, Z., Lin, Z., 2019. Foundations of offshore wind turbines: a review. Renew. Sustain. Energy Rev. 104, 379–393.